

# Surface Functionalization of Carbon Dots with Polyhedral Oligomeric Silsesquioxane (POSS) for Multifunctional Applications

Dan Wang, Jiangyong Liu, Jian-Feng Chen,\* and Liming Dai\*

Carbon dots (CDs), generally referring to small carbon nanoparticles with various levels of surface passivation,<sup>[1]</sup> have emerged as a new class of fluorescent nanomaterials attracting considerable attention in applications in bioimaging,<sup>[2]</sup> photovoltaics,<sup>[3]</sup> light-emitting devices,<sup>[4]</sup> catalysis,<sup>[5]</sup> etc.<sup>[6]</sup> Until now, CDs have been prepared through a number of methods including laser ablation, electrochemical oxidation, pyrolysis, or carbonization of organic precursors, which can be classified into two groups as top-down and bottom-up routes.<sup>[7]</sup> CDs synthesized via either of the synthetic routes usually contain many carboxyl groups or hydroxyl groups at their surfaces, enabling them to be subsequently functionalized with various organic, polymeric, inorganic, or biological species.<sup>[6d]</sup> By utilizing surface functionalization, one can significantly modify the optical properties of the CDs, while raw CDs exhibit weak emission in an aqueous medium or another solvent.<sup>[8]</sup> For instance, 4,7,10-trioxa-1,13-tridecanediamine (TTDDA),<sup>[9]</sup> oligomeric polyethylene glycol (PEG) diamine (PEG1500<sub>N</sub>),<sup>[8d,10]</sup> and polyethyleneimine<sup>[11]</sup> have been used as surface functionalization agents for CDs to increase their optical properties and solubility in aqueous solvents.

Polyhedral oligomeric silsesquioxane (POSS) is a hybrid inorganic/organic chemical composite which possesses an inner inorganic silicon and oxygen core and eight external organic arms.<sup>[12]</sup> The organic arms of POSS can be easily functionalized with organic pendant groups such as sulfhydryl, amino, carboxyl, and hydroxyl groups, which provide reactive sites for further functionalization. POSS derivatives have been shown to withstand a variety of thermal and chemical conditions,<sup>[13]</sup> and applied in many fields,<sup>[14]</sup> such as ion detection,<sup>[15]</sup> drug delivery,<sup>[16]</sup> and liquid marbles.<sup>[17]</sup> Very recently, octa(tetramethylammonium)-functionalized POSS (TMA-POSS) was used as a matrix to embed water-soluble CDs for the

fabrication of CD-based solid-state luminophores.<sup>[18]</sup> Wang et al. reported the use of octa-aminopropyl POSS hydrochloride salt (OA-POSS) as a passivation agent for preparation CDs/POSS hybrids and their applications in cell imaging.<sup>[19]</sup>

Here, we present the surface functionalization of water-soluble CDs with amine-functionalized POSS (POSS-NH<sub>2</sub>) by chemical bonding, imparting solubility of CDs in organic solvents. The obtained CDs@POSS nanocomposites exhibit enhanced photoluminescence and thermal stability compared to raw CDs, as well as superhydrophobic properties. The organic-soluble CDs@POSS hybrids have proven to be suitable for multifunctional applications, such as composite fillers, liquid marbles, and solid-state fluorescent sensors.

Figure 1a shows the schematic illustration of the route to synthesize CDs and CDs@POSS nanocomposites. The CDs were synthesized by hydrothermal treatment of citric acid solution in a Teflon autoclave, following a well-developed approach.<sup>[20]</sup> The amine-functionalized POSS molecule has eight organic pendant chains surrounding the cubic core, providing POSS with a high solubility in organic solvents. One end group of the eight organic chains is an amino group, allowing covalent grafting to CDs via the amide formation between the carboxylic acids and amines in the presence of *N,N'*-Dicyclohexylcarbodiimide (DCC). Therefore, the coverage of POSS on CDs depends on the ratio of POSS/carboxylic groups on the CDs. In our work, excess POSS molecules were used to fully cover the CDs with rich carboxylic groups. As shown in Figure 1b, the CDs dispersed well in water, which was attributed to the carboxylic moieties on the surfaces (Figure 1f, black line). The covalent bonding of CDs and POSS was evident by a phase transfer of CDs from the water phase into the CHCl<sub>3</sub> phase after the formation of CDs@POSS composites (Figure 1b,c). The obtained solution (CDs@POSS in CHCl<sub>3</sub>) exhibited a long-term homogeneous phase without any noticeable precipitation at room temperature. No major differences between the CDs and CDs@POSS were observed from TEM images, except for the latter being slightly larger and broader in size distribution according to statistical analysis (Figure 1d,e). A typical atomic force microscopy (AFM) image for CDs showed an average height of about 2 nm (Figure S1, Supporting Information). Upon the incorporation of POSS on CDs, the average height of CDs@POSS became 3.5 nm, which is higher than that of CDs (Figure S2, Supporting Information). The observed increase in size and thickness for CDs@POSS could be attributed to the surface coating of POSS on CDs. The FTIR spectra CDs@POSS (Figure 1e, red line) clearly showed the presence of a strong peak of characteristic Si–O–Si unit of the POSS cage at 1100 cm<sup>-1</sup> and relatively weak

Dr. D. Wang, Dr. J. Liu, Prof. J.-F. Chen  
State Key Laboratory of Organic-Inorganic Composites  
Beijing University of Chemical Technology  
Beijing 100029, China  
E-mail: chenjf@mail.buct.edu.cn

Dr. D. Wang, Dr. J. Liu, Prof. L. Dai  
Center of Advanced Science and Engineering for  
Carbon (Case4Carbon)  
Department of Macromolecular Science and Engineering  
Case School of Engineering  
Case Western Reserve University  
Cleveland, OH 44106, USA  
E-mail: liming.dai@case.edu



DOI: 10.1002/admi.201500439

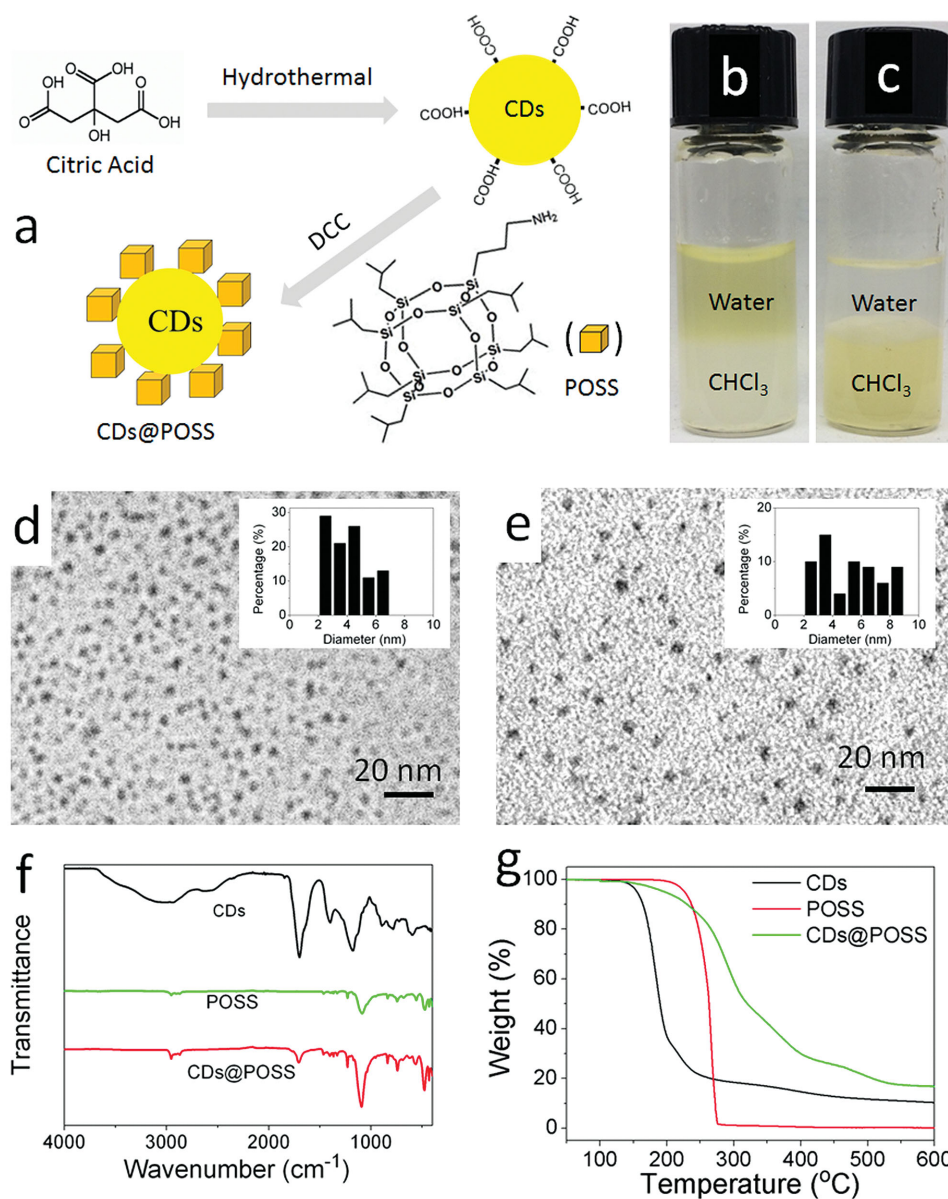


**Figure 1.** a) Schematic illustration of the route to synthesis of CDs and CDs@POSS; photographs of b) the CDs; and c) CDs@POSS in water/CHCl<sub>3</sub> solutions; typical TEM images of d) CDs and e) CDs@POSS, the inset histograms present the size distributions of the dots measured by TEM; f) FTIR spectra and g) TGA curves of CDs, POSS, and CDs@POSS.

bands over 2750–3000 cm<sup>-1</sup> associated with the isobutyl groups in POSS. The decreased peaks of hydroxyl (3470 cm<sup>-1</sup>), epoxy (1293 cm<sup>-1</sup>), and carbonyl (1703 cm<sup>-1</sup>) groups from CDs@POSS compared with those from CDs further demonstrated the chemical bonding of CDs and POSS. According to X-ray powder diffraction (XRD) results (Figure S3a, Supporting Information), CDs showed a broad peak centered at around  $2\theta = 25^\circ$ , which was attributed to highly disordered carbon atoms.<sup>[21]</sup> Characteristic XRD peaks of POSS were observed from CDs@POSS, indicating that the POSS crystal structure did not change after being covalently bonded to CDs (Figure S3b,c, Supporting Information). The thermal stability of CDs, POSS, and CDs@POSS was measured by TGA at a heating rate of 10 °C min<sup>-1</sup> under a nitrogen atmosphere (Figure 1g). A significant 60%

weight loss for CDs was observed at  $\approx 200$  °C, presumably due to the thermal desorption of water molecules physically adsorbed onto the hydrophilic and loss of oxygen-containing groups, while a complete weight loss was observed for POSS at  $\approx 200$  °C, presumably due to thermal evaporation. The CDs@POSS showed a better thermal stability than CDs with regards to both the temperature at the maximum rate of weight loss (290 °C) and the residual weight. The residual weight of CDs@POSS at 600 °C (17%) is higher than the CDs (10%), which can be attributed to the highly dense Si–O structure formed by the partial cross-linking of POSS.

Photoluminescence is one of the most important features of CDs, which makes them useful for fluorescence sensing, imaging, and light-emitting devices<sup>[4d]</sup> As shown in **Figure 2a**,

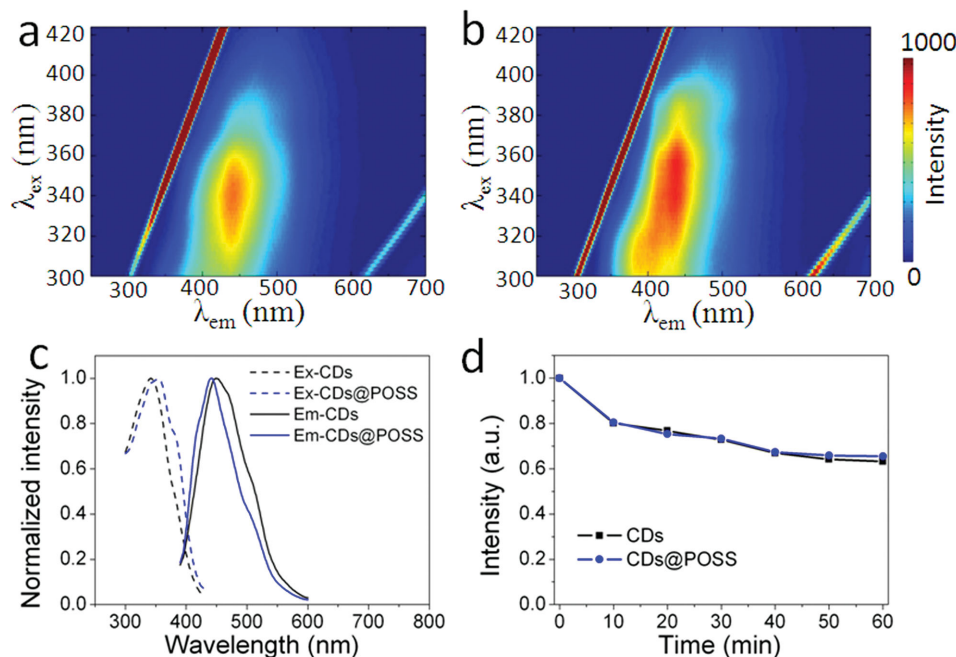


**Figure 2.** Photoluminescence excitation–emission maps of a) CDs and b) CDs@POSS, two trains of strong signals indicated by dashed white lines are due to scattering of excitation light and its second order; c) photoluminescence excitation and emission spectra of CDs in water and CDs@POSS in  $\text{CHCl}_3$ , respectively; d) normalized photoluminescence intensity of CDs and CDs@POSS under continuous UV irradiation at different times.

the CDs presented strong emission with excitation light in the range of 300–380 nm, and the maximum wavelength of emission is constant at  $\approx 445$  nm. The CDs@POSS exhibited similar photoluminescence excitation–emission map with that of CDs (Figure 2b). However, the emission intensity at respective excitation wavelength was higher than that of CDs. The relative fluorescence quantum yield of CDs excited with 350 nm UV light was calculated to be 6.4% by using the quinine sulfate as standard.<sup>[6d]</sup> This result is consistent with those of CDs previously reported in literatures.<sup>[20,22]</sup> Due to surface passivation of CDs in CDs@POSS, CDs@POSS nanocomposites exhibited a higher fluorescence quantum yield (10.2%) than bare CDs.<sup>[18,19,23]</sup> According to the respective normalized excitation spectra (emission at 450 nm wavelength) and emission spectra (excitation at 360 nm wavelength) of CDs and CDs@POSS solutions shown in Figure 2c, a slight blue shift of the photoluminescence maximum was observed for the CDs@POSS nanocomposites. This phenomenon is similar to that of silica-coated semiconductor quantum dots,<sup>[24]</sup> and we attributed it to the Si–O structure coating on the CDs and the difference of the solvents. The photostability of both CDs and CDs@POSS solutions was characterized by monitoring the photoluminescence intensity of the respective samples under continuous ultraviolet irradiation (365 nm UV lamp) for various times. As shown in Figure 2d, the luminescence intensities of CDs and CDs@POSS decreased in the initial 40 min and then remained stable. The decreased photoluminescence intensity of CDs suggested that part of the emission came from the organic molecule structures of CDs, which was damaged during the UV irradiation. Both CDs and CDs@POSS maintained 60% of photoluminescence intensity after continuous UV irradiation for up to 60 min.

The unique optical properties and good solubility of CDs@POSS in organic solvents make them ideal composite fillers for interfacial reinforcement with polymers. In this work, we chose poly(methyl methacrylate) (PMMA) as an example to study the potential functions and applications of CDs@POSS in polymer films. We prepared CDs@POSS/PMMA films by adding 1 wt% CDs@POSS into PMMA, and pure PMMA films were used as the reference. Figure 3a presents pictures of a PMMA film and a CDs@POSS/PMMA film under daylight and UV light, respectively. Both of the films were 1 mm thick and exhibited high transmission for visible light, as the letters under the films could be read clearly. However, the CDs@POSS/PMMA film showed bright blue emission while no emission was observed from the PMMA film under UV irradiation. The transmittance spectra and photoluminescence spectra of these two films are shown in Figure 3b,c, respectively. The decreased transmittance in the range of UV wavelength and the blue photoluminescence from CDs@POSS/PMMA were attributed to the optical absorbance and fluorescence of CDs@POSS, respectively. The thermal stability of a PMMA film and a CDs@POSS/PMMA film was investigated by TGA (Figure 3d). It can be seen that the decompose temperatures ( $T_d$ ) at 10 wt% loss were 296 and 303 °C for the PMMA film and CDs@POSS/PMMA film, respectively.

Another feature of CDs enabled by POSS functionalization was their superhydrophobicity. Figure 4a shows a water droplet (2  $\mu\text{L}$ ) on the surface of a CDs@POSS solid mass. The average water/air contact angle was measured to be 151.0°, indicating the superhydrophobicity of the surface.<sup>[25]</sup> As shown in the schematic illustration shown in Figure 4b, a liquid marble could be formed by coating the water droplet with

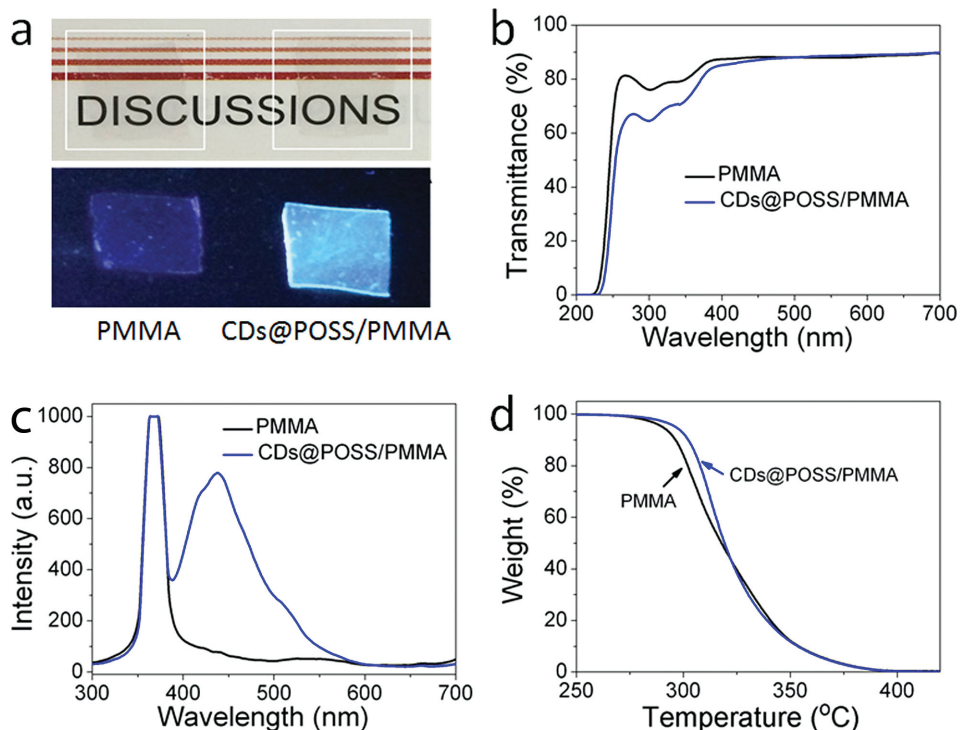


**Figure 3.** a) Digital photos of a PMMA film and a CDs@POSS/PMMA film (1 cm × 1 cm × 1 mm) under daylight and UV light, respectively; b) transmittance spectra; c) photoluminescence spectra; and d) TGA curves of a PMMA film and a CDs@POSS/PMMA film (2 cm × 1 cm × 1 mm), respectively.

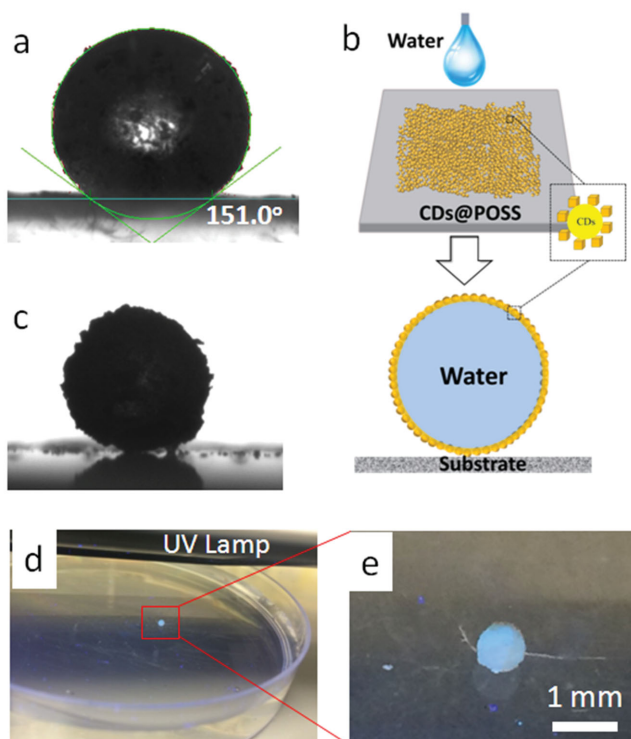


**Figure 4.** a) A water droplet (2  $\mu$ L) on the CDs@POSS film; b) schematic illustration of the formation of a CDs@POSS liquid marble; c) a CDs@POSS liquid marble on a glass surface; d) a CDs@POSS liquid marble floating on the surface of water; and e) blue emission from the CDs@POSS liquid marble in (d) under UV light excitation.

superhydrophobic CDs@POSS powder. Figure 4c shows the image of a CDs@POSS based liquid marble with 2  $\mu$ L water inside. Similar to liquid marbles made from other materials, the CDs@POSS-based liquid marble can stand freely on solid surfaces (Figure 4c) or float on the surface of water (Figure 4d). More interestingly, the CDs@POSS-based liquid marbles provided fluorescence under UV excitation (Figure 4e). The CDs@POSS based liquid marbles may find wide potential applications in sensing and drug delivery.

Selective fluorescent sensing of specific ions based on CDs has attracted much attention in recent years.<sup>[26]</sup> As shown in Figure 5a, the fluorescence of CDs was effectively quenched by  $\text{Fe}^{3+}$ , which can be attributed to the complex formed by CDs and  $\text{Fe}^{3+}$  ions, and a similar phenomenon has been investigated in some studies.<sup>[27]</sup> Here, we developed a novel solid-state fluorescent sensor based on CDs@POSS and commonly available filter papers. The fluorescent sensor was prepared by dipping a piece of filter paper into CDs@POSS solutions (1 mg mL<sup>-1</sup> in  $\text{CHCl}_3$ ) for 30 s and then drying it in air. The fluorescence of CDs@POSS from CDs@POSS/filter paper was observed under UV light excitation and the fluorescence spectra is presented in Figure 5b. The morphologies of raw filter paper and CDs@POSS/filter paper were investigated by SEM, and CDs@POSS aggregates were observed from the surface CDs@POSS/filter paper (Figure S4, Supporting Information). Unlike the raw filter paper or filter paper dipped with water-soluble CDs, which absorb water very quickly, CDs@POSS/filter paper was much more hydrophobic with a water/air contact angle of 90° (Figure S5, Supporting Information). This feature enabled the CDs@POSS/filter paper to sense

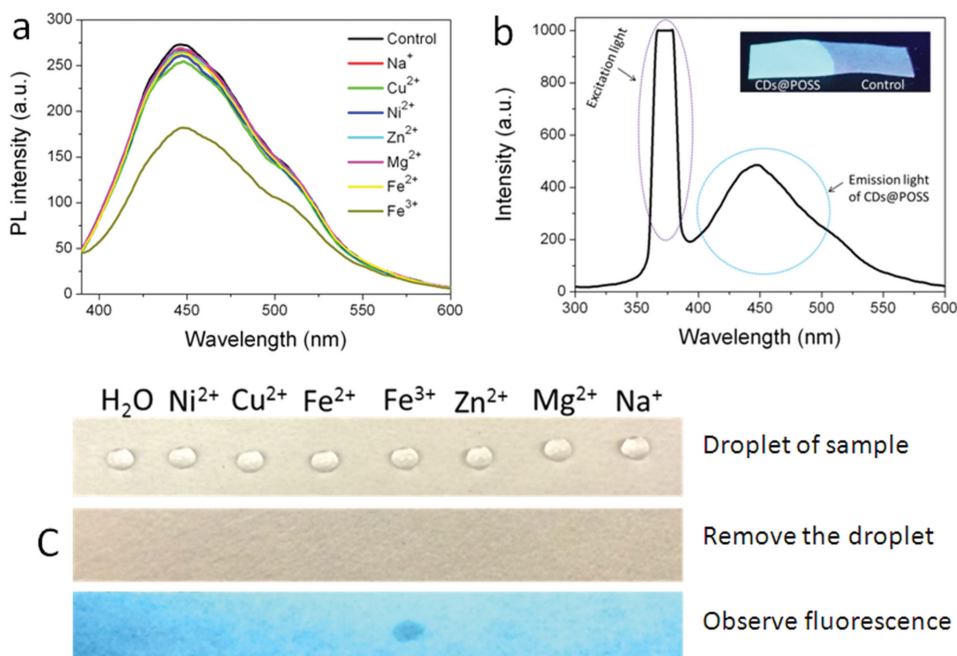


**Figure 5.** a) Fluorescence spectra of CDs solutions with the addition of various ions. The CDs concentration is  $1\mu\text{g mL}^{-1}$  and the concentration of each ion was  $10\text{ }\mu\text{M}$ ; b) photoluminescence spectra of CDs@POSS/filter paper; c)  $\text{Fe}^{3+}$  sensing by using CDs@POSS/filter paper as a solid-state fluorescent sensor.

several samples within a very small area (Figure S5, Supporting Information). Figure 5c shows the fluorescent sensing of  $\text{Fe}^{3+}$  by using a piece of CDs@POSS/filter paper. The concentration of the solution for each ion was  $10\text{ }\mu\text{M}$  in water and a droplet ( $2\text{ }\mu\text{L}$ ) of each sample was put on the surface of the sensor. After being maintained for 30 s, the droplets were removed and a UV lamp was used to excite the sensor. Clearly identifiable  $\text{Fe}^{3+}$  ions were observed with the naked eye, according to the decreased fluorescence intensity. The fluorescence quenching of CDs@POSS by  $\text{Fe}^{3+}$  can be attributed to the complexes between  $\text{Fe}^{3+}$  ions and CDs@POSS, as shown in the illustration in Figure S6 (Supporting Information).<sup>[26]</sup> Although the sensitivity of our solid-state fluorescent sensor is lower than that of fluorescence sensing in solutions, the novel fluorescent sensor may find applications in qualitative analysis due to their easy fabrication and useability.

In conclusion, we have successfully functionalized the CDs with POSS by covalent bonding, which was confirmed by TEM, AFM, XRD, FTIR, and TGA. The POSS structures grafted on CDs impart enhanced photoluminescence, thermal stability, and superhydrophobic properties to the CDs@POSS nanocomposites. We have demonstrated the applications of using CDs@POSS as composite fillers in PMMA, which can provide photoluminescence, enhanced UV absorbance and decomposed temperature. The superhydrophobic CDs@POSS powder can be used to prepare fluorescent liquid marbles for potential applications. A novel solid-state fluorescent sensor for  $\text{Fe}^{3+}$  fabricated by using CDs@POSS and commonly available filter papers was also presented in this work. We believe the newly developed CDs@POSS nanocomposites are promising for multifunctional applications in many fields.

## Supporting Information

Supporting Information is available from the Wiley Online Library or from the author.

## Acknowledgements

The authors are grateful for financial support from the “111” project of China (Grant No. B14004), the Beijing Municipal Science and Technology Project (Z151100003315005), and the open-funding program of the State Key Laboratory of Organic-Inorganic Composites.

Received: August 13, 2015

Revised: September 8, 2015

Published online: October 26, 2015

- [1] P. G. Luo, S. Sahu, S. T. Yang, S. K. Sonkar, J. Wang, H. Wang, G. E. LeCroy, L. Cao, Y.-P. Sun, *J. Mater. Chem. B* **2013**, *1*, 2116.
- [2] a) L. Cao, X. Wang, M. J. Meziani, F. S. Lu, H. F. Wang, P. J. G. Luo, Y. Lin, B. A. Harruff, L. M. Veca, D. Murray, S. Y. Xie, Y. P. Sun, *J. Am. Chem. Soc.* **2007**, *129*, 11318; b) W. Li, Z. Zhang, B. Kong, S. Feng, J. Wang, L. Wang, J. Yang, F. Zhang, P. Wu, D. Zhao, *Angew. Chem. Int. Ed.* **2013**, *52*, 8151; c) D. Wang, J.-F. Chen, L. Dai, *Part. Part. Syst. Character.* **2015**, *32*, 515; d) D. Wang, L. Zhu, J.-F. Chen, L. Dai, *Nanoscale* **2015**, *7*, 9894; e) E. V. Skorb, H. Möhwald, *Adv. Mater. Interfaces* **2014**, *1*, 1400237.
- [3] a) V. Gupta, N. Chaudhary, R. Srivastava, G. D. Sharma, R. Bhardwaj, S. Chand, *J. Am. Chem. Soc.* **2011**, *133*, 9960; b) P. Mirtchev, E. J. Henderson, N. Soheilnia, C. M. Yip, G. A. Ozin, *J. Mater. Chem.* **2012**, *22*, 1265; c) J. Briscoe, A. Marinovic, M. Sevilla, S. Dunn, M. Titirici, *Angew. Chem. Int. Ed.* **2015**, *54*, 4463.
- [4] a) X. Guo, C.-F. Wang, Z.-Y. Yu, L. Chen, S. Chen, *Chem. Commun.* **2012**, *48*, 2692; b) X. Y. Zhang, Y. Zhang, Y. Wang, S. Kalytchuk,

- S. V. Kershaw, Y. H. Wang, P. Wang, T. Q. Zhang, Y. Zhao, H. Z. Zhang, T. Cui, Y. D. Wang, J. Zhao, W. W. Yu, A. L. Rogach, *ACS Nano* **2013**, *7*, 11234; c) C. Sun, Y. Zhang, Y. Wang, W. Liu, S. Kalytchuk, S. V. Kershaw, T. Zhang, X. Zhang, J. Zhao, W. W. Yu, A. L. Rogach, *Appl. Phys. Lett.* **2014**, *104*, 261106; d) X. Li, Y. Liu, X. Song, H. Wang, H. Gu, H. Zeng, *Angew. Chem. Int. Ed.* **2015**, *54*, 1759.
- [5] H. Li, X. He, Z. Kang, H. Huang, Y. Liu, J. Liu, J. Liu, S. Lian, C. H. A. Tsang, X. Yang, S. T. Lee, *Angew. Chem. Int. Ed.* **2010**, *49*, 4430.
- [6] a) S. N. Baker, G. A. Baker, *Angew. Chem. Int. Ed.* **2010**, *49*, 6726; b) S. Y. Lim, W. Shen, Z. Gao, *Chem. Soc. Rev.* **2015**, *44*, 362; c) X. Li, M. Rui, J. Song, Z. Shen, H. Zeng, *Adv. Funct. Mater.* **2015**, *25*, 4929; d) X. Li, S. Zhang, S. A. Kulinich, Y. Liu, H. Zeng, *Sci. Rep.* **2014**, *4*, 4976; e) M. Favaro, S. Leonardi, C. Valero-Vidal, S. Nappini, M. Hanzlik, S. Agnoli, J. Kunze-Liebhäuser, G. Granozzi, *Adv. Mater. Interfaces* **2015**, *2*, 1400462.
- [7] H. Li, Z. Kang, Y. Liu, S.-T. Lee, *J. Mater. Chem.* **2012**, *22*, 24230.
- [8] a) L. Cao, M. J. Meziani, S. Sahu, Y. P. Sun, *Acc. Chem. Res.* **2013**, *46*, 171; b) X. Xu, R. Ray, Y. Gu, H. J. Ploehn, L. Gearheart, K. Raker, W. A. Scrivens, *J. Am. Chem. Soc.* **2004**, *126*, 12736; c) S.-T. Yang, X. Wang, H. Wang, F. Lu, P. Luo, L. Cao, M. J. Meziani, J.-H. Liu, Y. Liu, M. Chen, Y. Huang, Y.-P. Sun, *J. Phys. Chem. C* **2009**, *113*, 18110; d) X. Wang, L. Cao, S. T. Yang, F. Lu, M. J. Meziani, L. Tian, K. W. Sun, M. A. Bloodgood, Y. P. Sun, *Angew. Chem. Int. Ed.* **2010**, *49*, 5310.
- [9] H. Peng, J. Travas-Sejdic, *Chem. Mater.* **2009**, *21*, 5563.
- [10] L. Cao, S. T. Yang, X. Wang, P. G. Luo, J. H. Liu, S. Sahu, Y. Liu, Y. P. Sun, *Theranostics* **2012**, *2*, 295.
- [11] a) Y. Wang, P. Anilkumar, L. Cao, J.-H. Liu, P. G. Luo, K. N. Tackett II, S. Sahu, P. Wang, X. Wang, Y.-P. Sun, *Exp. Biol. Med.* **2011**, *236*, 1231; b) B. Han, W. Wang, H. Wu, F. Fang, N. Wang, X. Zhang, S. Xu, *Colloids and Surfaces B* **2012**, *100*, 209; c) X. Liu, H. J. Liu, F. Cheng, Y. Chen, *Nanoscale* **2014**, *6*, 7453; d) C. Wang, Z. Xu, C. Zhang, *ChemNanoMat* **2015**, *1*, 122.
- [12] a) S. W. Kuo, F. C. Chang, *Prog. Polym. Sci.* **2011**, *36*, 1649; b) Y. Xue, Y. Liu, F. Lu, J. Qu, H. Chen, L. Dai, *J. Phys. Chem. Lett.* **2012**, *3*, 1607; c) H. Hou, Y. Gan, J. Yin, X. Jiang, *Adv. Mater. Interfaces* **2014**, *1*, 1400385; d) H. Wang, H. Zhou, H. Niu, J. Zhang, Y. Du, Tong Lin, *Adv. Mater. Interfaces* **2015**, *2*, 1400506.
- [13] J. B. Carroll, A. J. Waddon, H. Nakade, V. M. Rotello, *Macromolecules* **2003**, *36*, 6289.
- [14] G. Li, L. Wang, N. Hanli, C. U. Pittman Jr., *J. Inorg. Organomet. Polym.* **2001**, *11*, 123.
- [15] a) F. Du, Y. Bao, B. Liu, J. Tian, Q. Li, R. Bai, *Chem. Commun.* **2013**, *49*, 4631; b) X. Zhao, J. Du, Y. Wu, H. Liu, X. Hao, *J. Mater. Chem. A* **2013**, *1*, 11748.
- [16] a) C. McCusker, J. B. Carroll, V. M. Rotello, *Chem. Commun.* **2005**, *8*, 996; b) H. Yuan, K. Luo, Y. Lai, Y. Pu, B. He, G. Wang, Y. Wu, Z. Gu, *Mol. Pharm.* **2010**, *7*, 953.
- [17] Y. Xue, H. Wang, Y. Zhao, L. Dai, L. Feng, X. Wang, T. Lin, *Adv. Mater.* **2010**, *22*, 4814.
- [18] Y. Wang, S. Kalytchuk, L. Wang, O. Zhovtiuk, K. Cepe, R. Zboril, A. L. Rogach, *Chem. Commun.* **2015**, *51*, 2950.
- [19] W. Wang, X. Hai, Q. Mao, M. Chen, J. Wang, *ACS Appl. Mater. Interfaces* **2015**, *7*, 16609.
- [20] S. Zhu, Q. Meng, L. Wang, J. Zhang, Y. Song, H. Jin, K. Zhang, H. Sun, H. Wang, B. Yang, *Angew. Chem. Int. Ed.* **2013**, *52*, 3953.
- [21] a) D. Y. Pan, J. C. Zhang, Z. Li, M. H. Wu, *Adv. Mater.* **2010**, *22*, 734; b) Y. Li, Y. Hu, Y. Zhao, G. Shi, L. Deng, Y. Hou, L. Qu, *Adv. Mater.* **2011**, *23*, 776; c) L. Tang, R. Ji, X. Cao, J. Lin, H. Jiang, X. Li, K. S. Teng, C. M. Luk, S. Zeng, J. Hao, S. P. Lau, *ACS Nano* **2012**, *6*, 5102.
- [22] Y. Dong, H. Pang, H. B. Yang, C. Guo, J. Shao, Y. Chi, C. M. Li, T. Yu, *Angew. Chem. Int. Ed.* **2013**, *52*, 7800.
- [23] F. Wang, Z. Xie, H. Zhang, C. Liu, Y. Zhang, *Adv. Funct. Mater.* **2011**, *21*, 1027.
- [24] D. Wang, J. Qian, F. Cai, S. He, S. Han, Y. Mu, *Nanotechnology* **2012**, *23*, 245701.
- [25] a) T. Darmanin, F. Guittard, *Adv. Mater. Interfaces* **2015**, *2*, 1500081; b) L. Xu, X. Lu, M. Li, Q. Lu, *Adv. Mater. Interfaces* **2014**, *1*, 1400011; c) H. Teisala, M. Tuominen, J. Kuusipalo, *Adv. Mater. Interfaces* **2014**, *1*, 1300026.
- [26] a) H. Li, J. Zhai, X. Sun, *Langmuir* **2011**, *27*, 4305; b) H. Li, J. Zhai, J. Tian, Y. Luo, X. Sun, *Biosens. Bioelectron.* **2011**, *26*, 4656; c) L. Zhou, Y. Lin, Z. Huang, J. Ren, X. Qu, *Chem. Commun.* **2012**, *48*, 1147; d) X. Shao, H. Gu, Z. Wang, X. Chai, Y. Tian, G. Shi, *Anal. Chem.* **2013**, *85*, 418; e) Z. Yang, Z. Li, M. Xu, Y. Ma, J. Zhang, Y. Su, F. Gao, H. Wei, L. Zhang, *Nano-Micro Lett.* **2013**, *5*, 247.
- [27] a) Y. Zhang, L. Wang, H. Zhang, Y. Liu, H. Wang, Z. Kang, S.-T. Lee, *RSC Adv.* **2013**, *3*, 3733; b) K. Qu, J. Wang, J. Ren, X. Qu, *Chem. Eur. J.* **2013**, *19*, 7243; c) J. Xu, Y. Zhou, G. Cheng, M. Dong, S. Liu, C. Huang, *Luminescence* **2015**, *30*, 411; d) X. Gong, W. Lu, M. C. Paau, Q. Hu, X. Wu, S. Shuang, C. Dong, M. M.F. Choi, *Anal. Chim. Acta* **2015**, *861*, 74.